

Origin of the prepeak in the structure factors of liquid and amorphous Al-Fe-Ce alloys

This article has been downloaded from IOPscience. Please scroll down to see the full text article.

1999 J. Phys.: Condens. Matter 11 7959

(<http://iopscience.iop.org/0953-8984/11/41/301>)

View [the table of contents for this issue](#), or go to the [journal homepage](#) for more

Download details:

IP Address: 171.66.16.214

The article was downloaded on 15/05/2010 at 13:24

Please note that [terms and conditions apply](#).

Origin of the prepeak in the structure factors of liquid and amorphous Al–Fe–Ce alloys

Zhang Lin, Wu Youshi, Bian Xiufang, Li Hui, Wang Weimin, Li Jingguo and Lun Ning

College of Materials Science and Engineering, Shandong University of Technology, Jinan 250061, People's Republic of China

Received 16 March 1999

Abstract. Distinct prepeaks have been found in the structure factors of the liquid and amorphous Al–Fe–Ce alloys. The structural size of the chemical short-range order corresponding to the prepeak in the liquid alloy increases with decreasing temperature, and, after glass forming, the structural size is much bigger, and the amount of the structure corresponding to the prepeak increases with decreasing quenching temperature, but the structural unit size remains constant. The position of the prepeak shifts to smaller Q -values as the concentration of Ce increases. The addition of Ce can improve the interaction between atoms, so it is favourable to Al-based glass formability. The structural unit corresponding to the prepeak is an icosahedral quasicrystalline structure with Fe as the interstitial atom, and the prepeak is diffraction peak broadening caused by fairly fine (about 0.5–2.0 nm) icosahedral clusters.

1. Introduction

A recently discovered group of Al–TM–RE (TM = transition metal, RE = rare earth metal) metallic glasses with aluminium content up to 90 at.%, such as $\text{Al}_{87}\text{Ni}_5\text{Y}_8$, $\text{Al}_{90}\text{Fe}_5\text{Ce}_5$ and $\text{Al}_{87}\text{Fe}_{8.7}\text{Gd}_{4.3}$, show excellent strength per weight, or specific strength [1–3]. It is unusual, however, that metallic glasses with such high concentrations of the primary element, in this case Al, can be formed by rapid quenching, since they most often fail to satisfy the atomic size criterion for glass formability [4]. Recent interest has centred on the origin of aluminium-based glass formability. The atomic structure of Al-based metallic glasses was studied by pulsed neutron scattering [5], x-ray scattering [6] and more recently EXAFS [7]. The results are all consistent. The main peak of the radial distribution function (RDF) of Al-based metallic glasses can be fitted by three Gaussian functions corresponding to the correlations between atoms, which point to strong covalent bonding between Al and TM. Since the Al coordination around TM atom is 6–7, the TM atoms are surrounded by about ten Al atoms with six of them being in close contact with TM. However, the RDF is a mean statistical function, and cannot reflect the strong local compositional order and geometrical order. The function of TM has been overemphasized, but the effects of RE on Al-based glass formability have been virtually ignored, so the origin of Al-based glass formability is still not very clear.

In this work, the effects of the liquid structure and quenching conditions on the microstructure of the Al–Fe–Ce amorphous alloys have been investigated. A prepeak in the structure factor of $\text{Al}_{90}\text{Fe}_5\text{Ce}_5$ melt with position similar to the prepeak position of $\text{Al}_{90}\text{Fe}_5\text{Ce}_5$ amorphous alloy, hitherto not mentioned in the literature, has been observed. The physical origin of the prepeak is not as yet clearly understood. In general, the presence of a prepeak corresponds

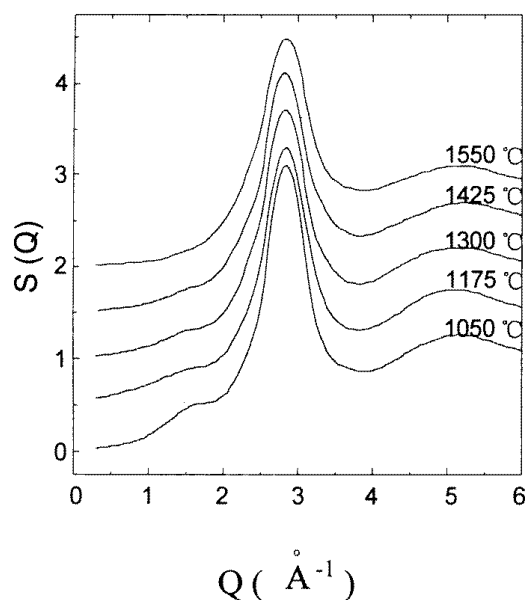


Figure 1. The total structure factors of liquid $\text{Al}_{90}\text{Fe}_{10}$ alloy at different temperatures.

to compound-forming behaviour [8], or can be attributed to cluster structure constituted of unlike atoms [9]. The similarity between the structure factor in the liquid and in the amorphous alloys implies that Al-based metallic glasses might inherit the composition fluctuation from the melt, which is favourable to determine the origin of Al-based glass formability.

2. Experimental procedure

Ingots of $\text{Al}_{90}\text{Fe}_5\text{Ce}_5$ were obtained from high purity elements in an arc furnace under argon atmosphere. Amorphous ribbons were prepared by the single roller melt-spinning technique under a partial argon atmosphere. The diameter of the copper roller was 35 cm, with a typical circumferential velocity of 40 m s^{-1} . The ribbons were $\sim 2 \text{ mm}$ in width and $\sim 25 \mu\text{m}$ in thickness.

The liquid and amorphous alloys have been investigated with x-ray wide-angle scattering, using a θ - θ diffractometer (2θ is the scattering angle) and Mo $K\alpha$ radiation selected by a diffracted beam focusing graphite monochromator. The liquid specimens were prepared in a crucible made of Al_2O_3 of size $8 \times 25 \times 30 \text{ mm}^3$ in high purity helium atmosphere, and measurements were carried out at the constant temperature $1550 \text{ }^\circ\text{C}$ with an accuracy of $\pm 5 \text{ }^\circ\text{C}$. The scattering intensity measured in arbitrary units can be converted into the coherent scattering intensity per atom in electron units, using the generalized Krogh-Moe-Norman method [10] with the atomic scattering factor including the anomalous dispersion factor [11]. Compton scattering is also corrected using the values given by Cromer and Mann [12]. Then, the total structure factor $S(Q)$ can be obtained from the scattering intensity, where $Q = (4\pi/\lambda) \sin \theta$ is the magnitude of the scattering vector, λ being the wavelength [10]. To identify the position and height of the prepeak, a parabolic-like function $f(x) = ax^2 + bx^3$, in which b is often much smaller than a , was used to fit the small angle part of $S(Q)$. Separation of the prepeak is executed by $S(Q)$ minus the parabolic-like function [13].

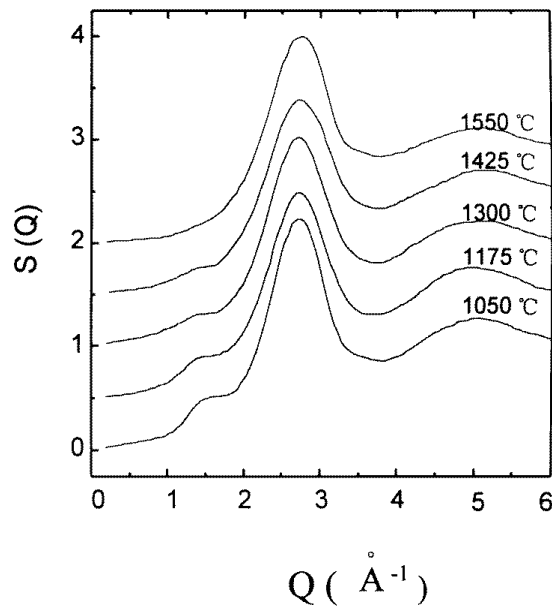


Figure 2. The total structure factors of liquid $\text{Al}_{90}\text{Fe}_5\text{Ce}_5$ alloy at different temperatures.

Thermal analysis was performed using a Netzsch DSC-404 system under a pure argon atmosphere.

3. Results

Figures 1 and 2 show the total structure factors of liquid $\text{Al}_{90}\text{Fe}_{10}$ and $\text{Al}_{90}\text{Fe}_5\text{Ce}_5$ alloys, respectively. The positions of the main peak and the prepeak are given in figure 3. The most interesting feature is the prepeak, which has been found at all investigated temperatures except 1550 °C. The prepeak and the main peak decrease their intensity with increasing temperature as expected for greater disorder. The prepeak and the main peak shift their positions towards smaller Q -values as 5 at.% Fe is substituted by Ce. Since the atomic radius of Ce is much bigger than those of Al and Fe, and the distance between atoms increases, it is reasonable to shift the peak position to smaller angle in reciprocal space. The main peak decreases its intensity with the addition of Ce because the size effect of the Ce atom causes the liquid structure much greater disorder. In the Al–Fe–Ce system, there are six independent pair correlations (Al–Al, Al–Fe, Al–Ce, Fe–Fe, Fe–Ce, Ce–Ce); however, only Al–Al, Al–Fe and Al–Ce correlations can exist in the alloy because of the low concentrations of Fe and Ce, and we can safely neglect the other three. The main peak corresponds to Al–Al correlation. Since the prepeak corresponds to strong interaction between unlike atoms [9], the prepeaks in liquid $\text{Al}_{90}\text{Fe}_{10}$ and $\text{Al}_{90}\text{Fe}_5\text{Ce}_5$ alloys can be attributed to the Al–Fe and Al–Ce correlations. The addition of Ce can increase the intensity of the prepeak, which indicates that Ce can increase the order of the structure corresponding to the prepeak and implies that the interaction between atoms has improved.

Figure 4 shows the total structure factors of amorphous $\text{Al}_{90}\text{Fe}_5\text{Ce}_5$ quenched at different temperatures. The positions of the main peak and the prepeak remain constant at different

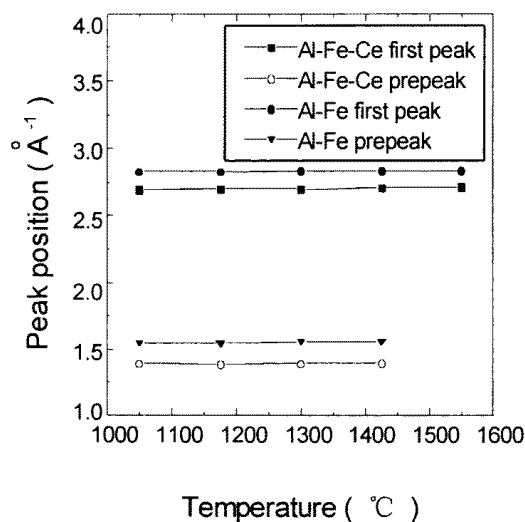


Figure 3. The positions of the main peak and the prepeak of liquid $\text{Al}_{90}\text{Fe}_{10}$ and $\text{Al}_{90}\text{Fe}_5\text{Ce}_5$ alloys.

quenching temperature, but the main peak and the prepeak increase their intensity with decreasing quenching temperature. A shoulder (or subpeak) on the main peak appears at scattering vector magnitudes of about 2.25 \AA^{-1} , which corresponds to the strong Al–Ce correlation [6], and the shoulder is weakened with increasing quenching temperature. This shows that the elevation of quenching temperature can decrease the composition fluctuation in the amorphous alloy. On the x-ray intensity curves, the ratio of the prepeak area (the integrated intensity of the diffraction curve) to the total area of the x-ray intensity curve can reflect the ratio of the structure corresponding to the prepeak in the matrix. Figure 5 shows $S_{\text{prepeak}}/S_{\text{total}}$ of amorphous $\text{Al}_{90}\text{Fe}_5\text{Ce}_5$ alloy quenched at different temperature. We may linearly extrapolate the prepeak area to that expected for the disappearance of the prepeak. The prepeak disappears at the quenching temperature of about $1557 \text{ }^\circ\text{C}$, which agrees with the x-ray diffraction result of liquid $\text{Al}_{90}\text{Fe}_5\text{Ce}_5$ alloy. At lower quenching temperature of $1050 \text{ }^\circ\text{C}$, only partial amorphous structure was obtained.

The prepeak corresponds to the cluster with short-range order, and each cluster contains several basic structural units. The structural unit size may be estimated according to a formula [14]: $R = 2\pi/Q_{pp}$, where R is a characteristic distance related to the structural unit size and Q_{pp} is the position of the prepeak. The structural unit sizes corresponding to the prepeaks of liquid $\text{Al}_{90}\text{Fe}_{10}$ and $\text{Al}_{90}\text{Fe}_5\text{Ce}_5$ alloys and amorphous $\text{Al}_{90}\text{Fe}_5\text{Ce}_5$ alloy are shown in figure 6. The structural unit sizes of $\text{Al}_{90}\text{Fe}_5\text{Ce}_5$ liquid and amorphous alloys are almost the same, which implies that the amorphous alloy might inherit the chemical short-range structure from the liquid alloy. The smallest structure unit size of liquid $\text{Al}_{90}\text{Fe}_{10}$ alloy indicates that the addition of Ce can improve the order of the structure. In addition, the structural unit size remains constant with changing temperature, further evidence for the covalently bonded stable structure existing in the liquid and amorphous alloys.

For estimations of the correlation length of the chemical short-range order structure, D (or the size of the cluster), a simple expression $D \approx 2\pi/\Delta Q$ (where ΔQ is the half-width of the prepeak) is often used [15, 16]. After separating the prepeak by the parabolic-like function, we used a Lorentzian approximation $S(Q) \sim \Delta Q/[Q - Q_{pp}]^2 + \Delta Q^2$ fitted to the small- Q side

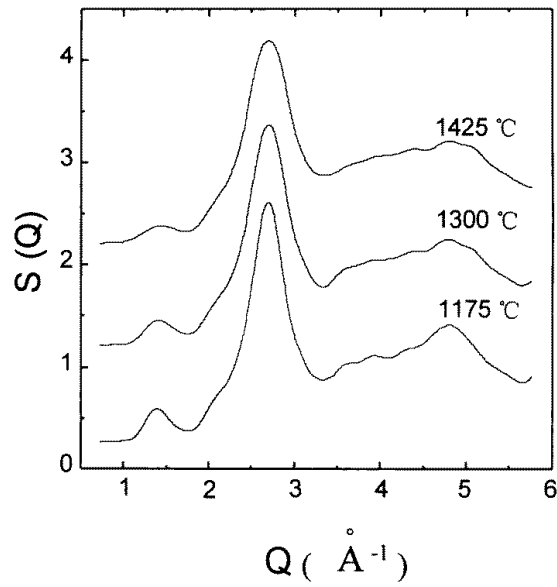


Figure 4. The total structure factors of amorphous $\text{Al}_{90}\text{Fe}_5\text{Ce}_5$ alloy quenched at different temperatures.

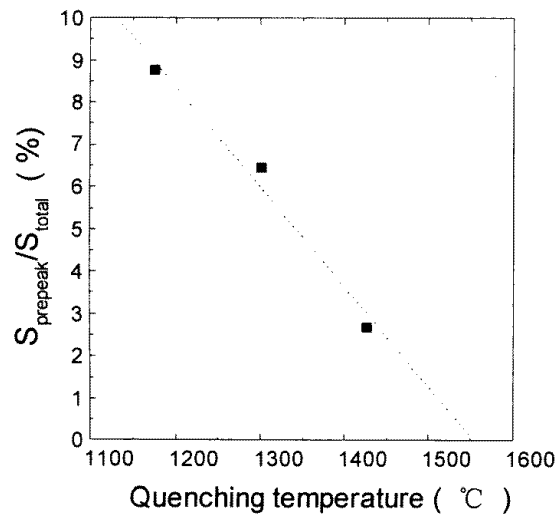


Figure 5. $S_{\text{prepeak}}/S_{\text{total}}$ of amorphous $\text{Al}_{90}\text{Fe}_5\text{Ce}_5$ alloy quenched at different temperatures.

of $S(Q)$ to evaluate the width ΔQ . Figures 7 and 8 show the half-width of the prepeak and the correlation length of liquid $\text{Al}_{90}\text{Fe}_{10}$ and $\text{Al}_{90}\text{Fe}_5\text{Ce}_5$ alloys and amorphous $\text{Al}_{90}\text{Fe}_5\text{Ce}_5$ alloy, respectively. The correlation length of the cluster structure corresponding to the prepeak increases with decreasing temperature and the correlation length of the amorphous alloy is much bigger than the others, in other words, the clusters corresponding to the prepeak grow with decreasing temperature or glass forming. In addition, the cluster size increases with the

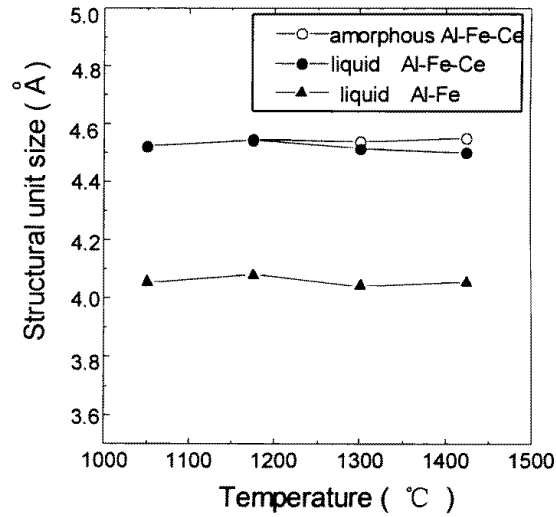


Figure 6. The structural unit sizes of liquid $\text{Al}_{90}\text{Fe}_{10}$ and $\text{Al}_{90}\text{Fe}_5\text{Ce}_5$ alloys and amorphous $\text{Al}_{90}\text{Fe}_5\text{Ce}_5$ alloy (the temperature for the amorphous alloy is the quenching temperature).

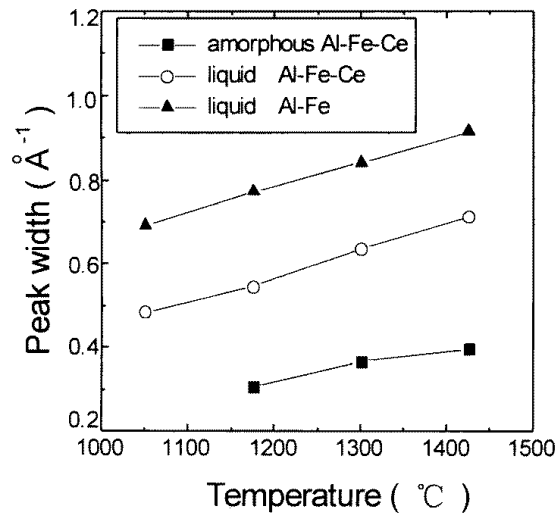


Figure 7. The half-width of the prepeak of liquid $\text{Al}_{90}\text{Fe}_{10}$ and $\text{Al}_{90}\text{Fe}_5\text{Ce}_5$ alloys and amorphous $\text{Al}_{90}\text{Fe}_5\text{Ce}_5$ alloy (the temperature for the amorphous alloy is the quenching temperature).

addition of Ce, and this also indicates that Ce can increase the order range by improving the interaction between atoms.

The DSC experiments were used to determine the crystallization process and the thermal stability of the amorphous alloys. DSC continuous heating curves for amorphous $\text{Al}_{90}\text{Fe}_5\text{Ce}_5$ alloy quenched at different temperatures are given in figure 9. At the quenching temperature of 1175°C , a exothermic peak is seen at 302.6°C with the crystallization activation energy of 247.7 mW ; at the quenching temperature of 1300°C , there are two exothermic peaks: the

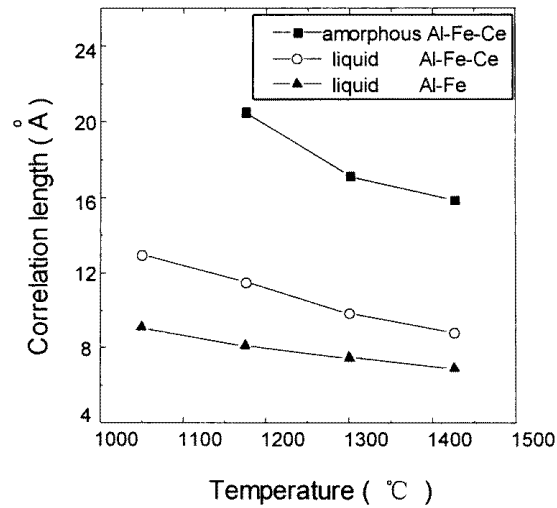


Figure 8. The correlation length of liquid $\text{Al}_{90}\text{Fe}_{10}$ and $\text{Al}_{90}\text{Fe}_5\text{Ce}_5$ alloys and amorphous $\text{Al}_{90}\text{Fe}_5\text{Ce}_5$ alloy (the temperature for the amorphous alloy is the quenching temperature).

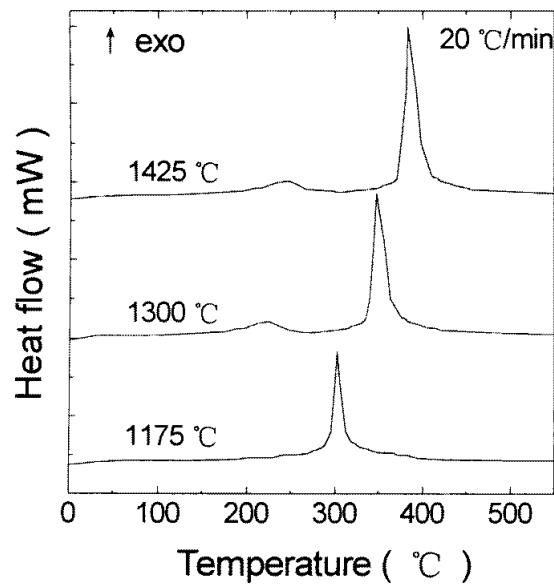


Figure 9. DSC curves for amorphous $\text{Al}_{90}\text{Fe}_5\text{Ce}_5$ alloy at different temperatures.

first peak is weaker and the second peak is found at 348.2°C with the crystallization activation energy of 333.69 mW ; at the quenching temperature of 1425°C , there are also two exothermic peaks, and the second peak is found at 383.8°C with the crystallization activation energy of 389.72 mW . The elevation of quenching temperature weakens the composition fluctuation in the amorphous alloy and increases the difficulty of crystallization. This also shows that the composition fluctuation in the melt increases with decreasing temperature.

Figure 10 shows the x-ray patterns at different temperatures of amorphous $\text{Al}_{90}\text{Fe}_5\text{Ce}_5$ alloy quenched at 1300°C . At ambient temperature, the microstructure of $\text{Al}_{90}\text{Fe}_5\text{Ce}_5$ alloy is all amorphous and a prepeak is found at the scattering angle of 19.5° ; at 250°C , the fcc-Al particles appear and the prepeak still exists; at 400°C , the sample is found to contain mostly Al phase and partial Al_4Ce , Al_3Fe and $\text{Al}_{10}\text{CeFe}_2$ compounds, the position of the prepeak corresponding to the $\text{Al}_4\text{Ce}(101)$ peak, the $\text{Al}_3\text{Fe}(112)$ peak and the $\text{Al}_{10}\text{CeFe}_2(200)$ peak. Therefore, the prepeak is related to the strong chemical bonds which cause compound forming.

4. Discussion

The prepeak is a distinct feature and represents a single Fourier component in reciprocal space, corresponding to a quasi-periodic arrangement of atoms in real space which extends over medium range (about 0.5–2.0 nm) [17]. The prepeaks in the total structure factors show that the chemical short-range order structure (or the structural unit) and the medium-range order structure (or the cluster) caused by strong Al–Fe and Al–Ce chemical bonds exist in the Al–Fe–Ce liquid and amorphous alloys. From the above experimental results, the addition of Ce increases the sizes of the cluster and its structural unit, Ce can increase the structure order by strengthening the chemical bonds between atoms, which causes the Al–Fe–Ce alloy to have a certain covalent characteristic and is favourable to Al-based glass formability. Figure 10 shows that the structure corresponding to the prepeak is much more stable than the Al matrix, and needs more crystallization activation energy. The Al matrix is metallic bonding between atoms, but the existence of the prepeak at 250°C is the sign of a strong chemical bond (covalent bond) which increases the difficulty of crystallization.

From figures 6 and 8, the cluster size in the liquid $\text{Al}_{90}\text{Fe}_5\text{Ce}_5$ alloy increases with decreasing temperature, and after glass forming the cluster will be much bigger, but the structural unit size of the cluster remains constant. This indicates that the amorphous alloy has basically retained the structural unit of the chemical short-range order in the liquid alloy; however, the correlation length of the structural unit has increased. The number of clusters in the amorphous alloy decreases with increasing quenching temperature, which also reflects that the composition fluctuation in the melt becomes weak with increasing temperature. The x-ray diffraction result of liquid $\text{Al}_{90}\text{Fe}_5\text{Ce}_5$ alloy at 1550°C agrees with the extrapolated quenching temperature for the disappearance of the prepeak. The DSC curves also show that the elevation of quenching temperature weakens the composition fluctuation in the amorphous alloy and increases the difficulty of crystallization. Therefore, it is thus evident that the size and number of clusters in the melt increases with the reduction of temperature, but the structural unit remains constant.

The discovery of quasiperiodic structures with icosahedral symmetry by Shechtman [18] has aroused interest in the study of short-range icosahedral order in liquid and amorphous alloy [19, 20]. Previously, the idea that structures of liquid metals could be based on packing of icosahedral units was suggested by Frank in order to explain supercooling affects [21]. Even though this property was later confirmed by dynamics simulations of supercooled liquids [22], experimental proof is still required. Recently, the results of the studies on liquid $\text{Al}_{80}\text{Mn}_{20}$ and $\text{Al}_{71}\text{Pd}_{19}\text{Mn}_{10}$ alloys [23, 24] suggest the presence of local icosahedral order in these liquid states, but no direct comparison has yet been made with the local order in the solid state. Here, the prepeak position of liquid $\text{Al}_{90}\text{Fe}_{10}$ alloy is in the close vicinity of one of the prominent diffraction peaks of the quasicrystalline Al–Fe(110001) reflection (at about 1.6 \AA^{-1}) [25]. This suggests that the chemical short-range order structure of liquid $\text{Al}_{90}\text{Fe}_{10}$ alloy might be similar to the quasicrystalline structure, and the clusters may be packed with some icosahedral short-range order. The prepeak position of $\text{Al}_{90}\text{Fe}_5\text{Ce}_5$ liquid and amorphous alloys (at about

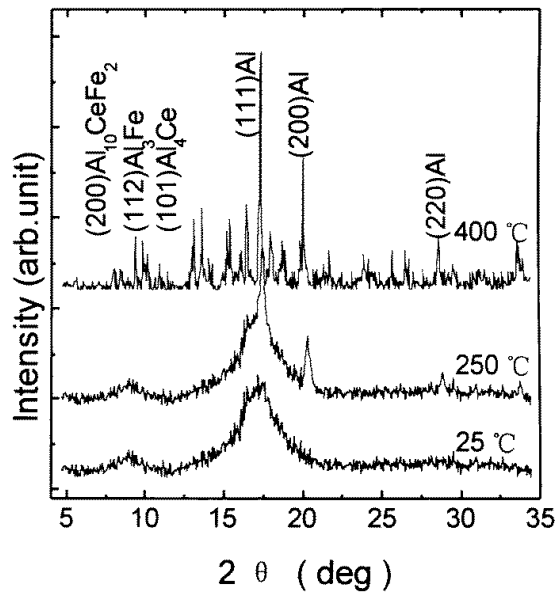


Figure 10. The x-ray patterns at different temperatures of amorphous $\text{Al}_{90}\text{Fe}_5\text{Ce}_5$ alloy.

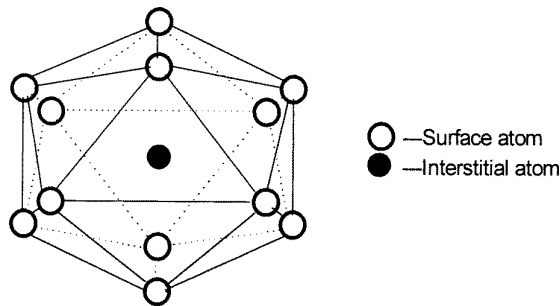


Figure 11. The scheme for the centred icosahedral structural unit $\partial^2G/\partial x^2$.

1.38 \AA^{-1}) is close to the $\text{Al}_{10}\text{CeFe}_2$ intermetallic compound (200) peak; in fact, $\text{Al}_{10}\text{CeFe}_2$ quasicrystalline icosahedral phase has been reported in rapidly cooled Al–Fe–Ce alloy [26], so it is possible to speculate that the structural units corresponding to the prepeaks of $\text{Al}_{90}\text{Fe}_{10}$ and $\text{Al}_{90}\text{Fe}_5\text{Ce}_5$ alloys may be both icosahedral short-range order structures, but the size effect of Ce atom shifts the prepeak position of $\text{Al}_{90}\text{Fe}_5\text{Ce}_5$ alloy towards smaller Q -values. It can be considered that the prepeak is diffraction peak broadening caused by fairly fine (about 0.5–2.0 nm) icosahedral clusters.

An icosahedron can be centred and composed of 13 atoms, as illustrated in figure 11. Because Fe and Ce atoms are in the minority, most of 12 atoms on the icosahedral shell are Al atoms. For convenience, we may presume that the atoms on the icosahedral shell are all Al atoms. Since the Al–Al distance is 0.286 nm, the Al–Ce distance is 0.325 nm, the Al–Fe distance is 0.249 nm (the reduction of Al–Fe distance is due to the strong orbital hybridization of the 3d states of Fe with the 3s and 3p states of Al) [6], with Al, Fe and Ce as the interstitial

atom, the maximum sizes for two orientations of the icosahedrons are $0.544 \text{ nm} \times 0.572 \text{ nm}$, $0.474 \text{ nm} \times 0.498 \text{ nm}$ and $0.618 \text{ nm} \times 0.650 \text{ nm}$, respectively. The structural unit corresponding to the prepeak in $\text{Al}_{90}\text{Fe}_5\text{Ce}_5$ alloy is about 0.455 nm , which is close to the icosahedron with Fe as the interstitial atom. Fe and Ce atoms on the icosahedral shell can increase the interaction between atoms, and reduce the distance between atoms, so this can make the calculated result agree with the experimental result. The icosahedral size shows that there are fewer Ce atoms than Fe atoms in the icosahedron because of the bigger atomic radius of Ce, and a shoulder on the main peak in the structure factor of amorphous $\text{Al}_{90}\text{Fe}_5\text{Ce}_5$ alloy which corresponds to the strong Al–Ce correlation also shows that there are more Ce atoms randomly distributed in Al matrix. The densest packing icosahedral structure with the smaller atom as the interstitial atom and the coordination number around it of 12 can exist stably in liquid and amorphous alloys, but it cannot exist in the crystalline materials with periodic arrangement of atoms [27]. A cluster can be described as several centred icosahedrons fused together via vertex, edge or plane sharing [28, 29]. In liquid alloys a cluster is constituted by 4–9 icosahedral structural units, and in amorphous alloys a cluster is constituted by 10–6 icosahedral structural units. Therefore, amorphous $\text{Al}_{90}\text{Fe}_5\text{Ce}_5$ alloy is composed of the clusters with the icosahedral short-range order structure and the amorphous Al matrix.

In accordance with the spinodal decomposition theory given by Cahn [30], a model of the transition from liquid to glass can be constructed. Above $1550 \text{ }^\circ\text{C}$, $(\partial^2 G/\partial x^2) > 0$, where G is free energy; x is the composition of Fe or Ce, the liquid Al–Fe–Ce alloy is a homogeneous single phase at equilibrium; below $1550 \text{ }^\circ\text{C}$, $(\partial^2 G/\partial x^2) < 0$, the strong chemical bonds cause weak fluctuation or small separation in composition in order to decrease free energy, which has the characteristic of the early stages of spinodal decomposition. Here, the cluster is the sign of composition fluctuation. The size of the cluster increases with the reduction of the melt temperature, and it is about 1 nm in the melt. The cluster contains strong chemical bonds and has a certain covalent characteristic, so it is stable and difficult to crystallize. Since the clusters crystallize later, they cannot become the crystal nuclei of the Al phase. However, the cluster size is much bigger than those of any other atoms, so the clusters can be regarded as ‘huge atoms’ which can cause great size effects in the matrix, prevent the Al matrix from crystallizing and improve the stability of the amorphous matrix. The clusters caused by strong chemical bonds make the Al–Fe–Ce alloy favourable to the Al-based glass formability. It is thus clear that the strong chemical short-range order corresponding to the prepeak in the Al–Fe–Ce alloy is the sign of strong chemical bonds existing which is the fundamental reason for Al-based glass formability.

5. Conclusions

From the x-ray diffraction and DSC experiments, especially from the observation of a prepeak in the structure factor, it may be concluded that the cluster size in the liquid Al–Fe–Ce alloy increases with decreasing temperature, and, after glass forming, the cluster will be much bigger, but the structural unit size of the cluster remains constant, which indicates that the amorphous alloy has basically retained the structural unit of the chemical short-range order in the liquid alloy, and the addition of Ce can increase the cluster size and its unit size, and improve the interaction between atoms, which causes the Al–Fe–Ce alloy to have a certain covalent characteristic and to be favourable to Al-based glass formability; in addition, the structural unit corresponding to the prepeak is an icosahedral quasicrystalline structure with Fe as the interstitial atom and the prepeak is diffraction peak broadening caused by fairly fine (about $0.5\text{--}2.0 \text{ nm}$) icosahedral clusters.

Acknowledgment

This work was supported by the National Natural Science Foundation of China (Project No 59671046).

References

- [1] He Y, Poon S J and Shiflet G J 1988 *Science* **241** 1640
- [2] Tsai A P, Inoue A and Masumoto T 1988 *J. Mater. Sci. Lett.* **7** 805
- [3] Tsai A P, Kamiyama T, Kawamura Y and Inoue A 1997 *Acta Mater.* **45** 1477
- [4] Egami T and Wasada Y 1984 *J. Non-Cryst. Solids* **64** 113
- [5] Hsieh H Y, Toby B H, Egami T and He Y 1990 *J. Mater. Res.* **5** 2807
- [6] Hsieh H Y, Egami T, He Y and Poon S J 1991 *J. Non-Cryst. Solids* **135** 248
- [7] Mansour A N, Wrong C P and Brizzolara R A 1991 *Phys. Rev. B* **50** 12 401
- [8] Matubara E, Harada K, Wasda Y, Chen H S and Inoue A 1988 *J. Mater. Sci.* **23** 753
- [9] Hoyer W and Jodicke R 1995 *J. Non-Cryst. Solids* **192–193** 102
- [10] Wasada Y 1989 *The Structure of Non-Crystalline Materials* (New York: McGraw-Hill)
- [11] Wasada Y 1974 *International Tables for X-ray Crystallography IV* ed C A MacCillavary *et al* (Birmingham: Kynoch)
- [12] Cromer D T and Mann J B 1967 *J. Chem. Phys.* **47** 1892
- [13] Salmon P S 1994 *Proc. R. Soc. A* **445** 351
- [14] Vateva E and Savova E 1995 *J. Non-Cryst. Solids* **192–193** 145
- [15] Sokolov A P, Kisliuk A and Soltwisch M 1992 *Phys. Rev. Lett.* **69** 1540
- [16] Borjesson L, Torell L M, Dohlborg U and Howels W S 1989 *Phys. Rev. B* **39** 3404
- [17] Elliott S R 1991 *Phys. Rev. Lett.* **67** T11
- [18] Shechtman D, Blech I, Gratias D and Cahn J W 1984 *Phys. Rev. Lett.* **53** 1951
- [19] Sachdev S and Nelson D R 1984 *Phys. Rev. Lett.* **53** 1947
- [20] Sachdev S and Nelson D R 1985 *Phys. Rev. B* **32** 4592
- [21] Frank F C 1952 *Proc. R. Soc. A* **215** 43
- [22] Steinhardt P J, Nelson D R and Ronchetti M 1983 *Phys. Rev. B* **28** 784
- [23] Maret M, Chieux P, Dubois J M and Pasturel A 1991 *J. Phys.: Condens. Matter* **3** 2801
- [24] Maret M, Lancon F and Billard L 1993 *J. Physique* **13** 1873
- [25] Dubois J M, Janot C, Pannetier J and Fruchart R 1987 *Key Eng. Mater.* **13–15** 271
- [26] Angers L M 1987 *Metall. Trans. A* **18** 555
- [27] Levine D and Steinhardt P J 1984 *Phys. Rev. Lett.* **53** 2477
- [28] Boon K T, Hong Zhang, Yin Kean and Hy Dang 1993 *J. Chem. Phys.* **99** 2929
- [29] Guo Kexin 1998 *Physica* **27** 515 (China)
- [30] Cahn J W 1961 *Acta Metall.* **10** 795